Chaos in Bird Vocalizations

A Senior Project submitted to
The Division of Science, Mathematics, and Computing
of
Bard College

by
Paul Samuel McLaughlin

Annandale-on-Hudson, New York
December, 2009

Abstract

Chaos is studied in terms of bird vocalizations. Zebra Finch song is analyzed for chaos using methods from non-linear dynamics. Mainly through recurrence analysis and delay plot analysis, it is shown that the aperiodic sections analyzed in the song are most likely exhibiting periodic behavior with added noise and are thus not chaotic. A model of the syrinx, the bird's sound production organ, is then analyzed for chaos. The model is found to exhibit chaotic behavior with feasible parameters for bird species previously found to be capable of producing chaotic vocalizations.

Contents

List of Figures

Dedication

For my family, Shelley and most of all my dogs Bubba, Buttercup and Vishi.

Acknowledgments

I would like to thank my adviser Jim Belk for all of the time, effort and enthusiasm he has put into this project. The incredible patience and wisdom he has shown me over the past year has not only encouraged me to strive to be a better mathematician but also a better person. It was truly an honor to work with him. I would also like to thank the other members of my board, Sven Anderson and Mary Krembs, for all of their suggestions, and for the time they have spent on my project. For all of the software help I thank Adina-Raluca Stoica. Finally, I would like to thank my friends from the computer lab for their invaluable help and distractions: Ezra, Natalie, Greg, Sylvia and Denise.

1
Introduction

Over the past three decades new advances in the theory of nonlinear dynamics have provided scientists with an abundance of tools for investigating dynamical systems. Many phenomena occurring in nature which had previously been classified as stochastic can now be shown to exhibit deterministic dynamic behavior [6]. One of these is the phenomena of birdsong.

Bird vocalizations have been the subject of study for many years, from acoustical, behavioral and physiological points of view [9]. In particular there has been a great deal of research into birds' muscle control and the sound production organ in birds known as the syrinx [4]. Birds have been found to have an impressive amount of versatility in creating a wide range of tones, including those which exhibit complex structure and high levels of overtones. Some species have even been found to produce chaotic calls [9]. This paper investigates this subject further.

First, through recurrence analysis, aperiodic data will be analyzed for determinism. Delay plots will also be used to determine whether this data is chaotic. Then there will be

an investigation into a model of the syrinx to verify if the model is capable of producing chaos and thus capable of modeling the impressive array of the bird's capabilities.

2
Preliminaries

2.1 Dynamical Systems

A **dynamical system** is a set of possible states and a rule which describes how one **state** evolves into another state over time. A state of a dynamical system is given by a real number, or a tuple of real numbers. A **deterministic** dynamical system is one in which the state of the system can be determined uniquely from the past states. This idea of a deterministic dynamical system can be seen in contrast to a random or **stochastic** system, where randomness is involved in the evolution process. For a general overview of dynamical systems see [2].

Both discrete and continuous dynamical systems will be discussed in this paper. A discrete dynamical system is evolved by iterating the map or set of maps which govern the system. A continuous dynamical system generally evolves according to a differential equation or set of differential equations.

Many dynamical systems are periodic, meaning the dynamical system is one in which a set of states is repeated in regular intervals of time. The **period** of a dynamical system is the amount of time it takes the system to move through all of these states. In a discrete

dynamical system, for instance, a system is said to have a period four if it takes four iterations for the system to return to the same state.

A good way of understanding how a dynamical system evolves is by viewing its **state space**. A state space (or phase space) for a system is a topological space in which each possible state is represented by a single point. Another good tool for analyzing dynamical systems is a **time series**. A time series constructed from a dynamical system is the set containing all ordered pairs $(x_t,\ t)$, where x_t represents one variable of the state of the dynamical system at time t. A limitation of a time series in comparison to a state space of a dynamical system is that only one variable of the system can be modeled with a time series. The problems caused by this limitation will be discussed further in proceeding sections.

2.2 Chaos

Chaos can be thought of as occurring somewhere in between periodic behavior and random behavior [9]. A chaotic system is a deterministic system which is none the less unpredictable. Chaotic systems exhibit sensitive dependence on initial conditions, which makes it very difficult to distinguish the long term behavior of the system from a stochastic process [2]. Many of the tests to distinguish data coming from a chaotic system as opposed to that coming from a stochastic system are based around recognizing the difference that arises between the short term behavior of the data due to chaotic systems being deterministic. An example of a chaotic system is given below.

Example 2.2.1. A simple example of a chaotic system is the system governed by the **logistic map**. The logistic map takes a point x_n and maps it to the new point

$$x_{n+1} = rx_n(1 - x_n)$$

The logistic map is known to exhibit chaotic behavior for many values of r between 3.57 and 4 [2], Figure 2.2.1 shows two versions of 200 iterations of the Logistic map with $r = 3.8$. The plot on the left has as its initial condition 0.8, and the plot on the right 0.8000000000005.

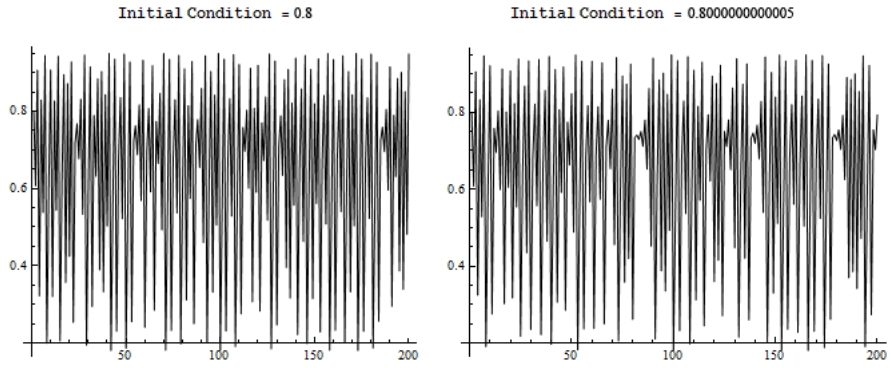

Figure 2.2.1. 200 iterations of the logistic map

This example helps illustrate that the long term behavior of a chaotic system can be very difficult to predict. Although the two initial conditions are within 0.000000000005 of one another, there is a significant difference between the two plots. This example is also quite remarkable when considering the fact that the behavior of the plot is being governed by such simple rules.

It can also be noticed that there appears to be short sections of quasi periodic behavior in both of the plots, and small segments with similar structure. An example of these segments with similar structure can be seen in the second plot immediately before the 100^{th} iteration and immediately before the 150^{th} iteration. Both of these characteristics come from the fact that the data was produced by a low-dimensional deterministic source. This topic will be discussed further in Section 3.1.1, and will be the underlying idea behind the recurrence analysis test which separates random data from deterministic.

2.2.1 Period Doubling

Another important characteristic of chaos that will be important when discussing the models of the bird's syrinx is **period doubling**. The time series of a chaotic dynamical system goes through period doubling or **bifurcations** when its parameters are approaching the values which produce chaos. An example of period doubling in the logistic map can be seen in Figure 2.2.2, where the period becomes increasingly more complicated as the value of r is increased to levels where it produces chaos. Because chaos often occurs after period doubling, it can be a very helpful indicator when searching for parameters which induce chaos in a certain dynamical system.

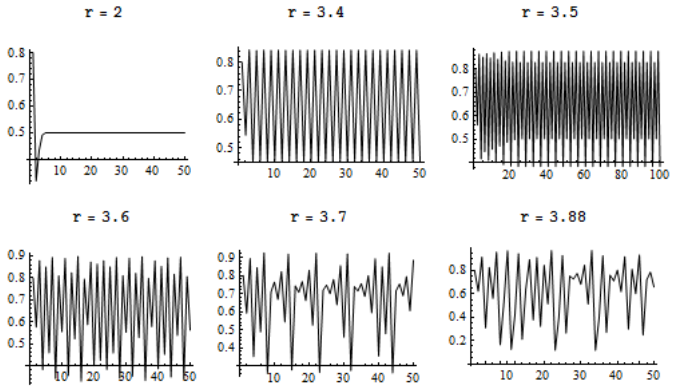

Figure 2.2.2. Period doubling and chaos in the logistic map

2.2.2 Chaos in Biological Data

When working with data generated from a real-world biological source compared to that from a mathematical model, some of the concepts need to be treated slightly differently. The most significant of the differences which must be discussed is that of real-world data which is quasi periodic. For instance, the time series data in Figure 2.2.3 shows what will be classified as a periodic birdsong in this paper. However, the data is not perfect, mathematically speaking. Because of the slight inconsistencies from perfect periodic behavior, this data would generally be classified as chaotic. Studying this data as chaotic may be

interesting from a mathematical standpoint, however it would do little for gaining insight into the actual system with which the birds are generating the vocalizations. Because of this fact, when studying the data coming from real birdsong, only deterministic data with no sign of long term periodic behavior will be considered as chaotic.

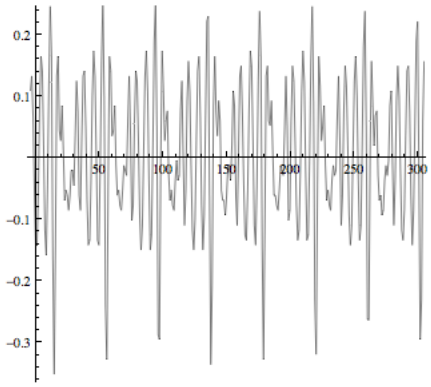

Figure 2.2.3. Periodic birdsong data

2.2.3 Chaotic Data from Multivariable Systems

Determining whether data is chaotic becomes increasingly difficult as the complexity of the system producing the data increases. The birdsong data discussed throughout this paper will come in the form of time series. Time series data however only provides one variable coming from the multivariable system of the syrinx. **Recurrence analysis** and **delay plot analysis**, discussed in Chapters 3 and 4, are techniques which will be used to help discern if the time series data came from a chaotic system.

An important concept which will arise when discussing delay plots is that of a **strange attractor**. A strange attractor is a fractal shape which attracts points in the state space. Two examples of strange attractors are given below.

Figure 2.2.4 shows the strange attractor in the state space of the system governed by the **Hénon map**. The Hénon map is defined as the map which takes the point $(x_n,\ y_n)$, and maps this point to the new point $(y_n - 1.4x_n^2 + 1,\ 0.3x_n)$ [7].

Figure 2.2.5 shows the strange attractor in the state space of the **Lorenz oscillator**. The Lorenz Oscillator is a known chaotic dynamical system made up of three coupled differential equations. The three equations are $\frac{dx}{dt} = \sigma(y - x)$, $\frac{dy}{dt} = x(\rho - z) - y$ and $\frac{dz}{dt} = xy - \beta z$ [2]. The parameters $\sigma = -3$, $\rho = 26.5$ and $\beta = 1$ were used.

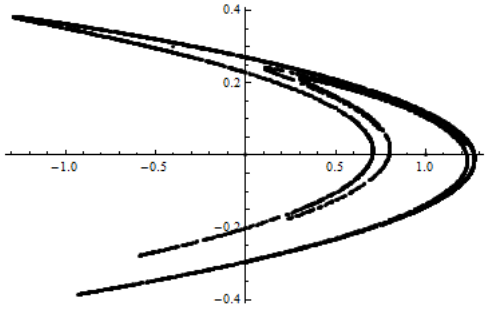

Figure 2.2.4. The attractor of the chaotic system governed by the Hénon map

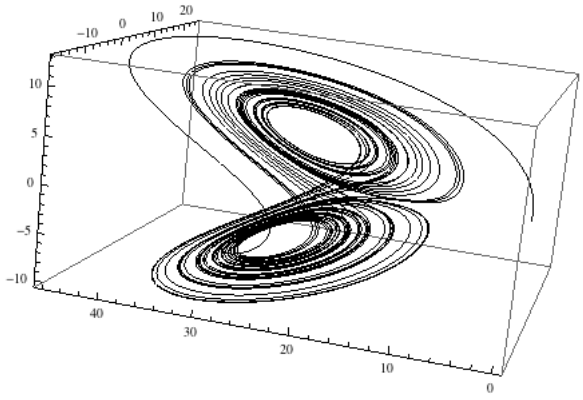

Figure 2.2.5. Lorenz attractor

2.3 Birds

2.3.1 Birdsongs

All of the real-world data analyzed in this paper were sections of birdsongs. For a brief introduction to birdsong see [13]. Birdsongs are vocalizations which are usually associated with mating rituals. Although there would not be a significant difference in the level on

which the birdsongs were analyzed for this research, there is usually a distinction made between birdsong and bird calls. Birdsongs are usually longer and more complex than bird calls. Bird calls are also usually associated with vocalizations pertaining to distress calls, or for keeping members of a flock in contact.

Another term that will come up within this paper is a **syllable** of a birdsong. A syllable is a section of birdsong separated by silence, or an abrupt change in frequency.

2.3.2 Data

The data that was primarily used in this project was of Zebra Finch songs. The main reason for this was due to the abundance of data that was available. The Zebra Finch also seemed like a good candidate because of the unpleasant nature of its song, which is characteristic of chaotic sound.

The song files were downloaded from Heather H. Williams' *Zebra Finch Song Archive* website [13]. There, Professor Williams, working through Williams College, has recorded and archived over 80 male Zebra Finches birdsongs. Along with the song and lineage of the individual bird, a **sonogram**, which is a plot of frequency versus time, of each song is listed. These were used to find songs containing syllables with a high number of different frequencies. Songs that display this property are more likely to exhibit chaos. The songs were then shortened to contain these selected syllables in Audacity, and these syllables were then visually analyzed to verify that they contained aperiodic sections. The syllables that did contain aperiodic sections were then imported into Mathematica.

2.3.3 Bird Anatomy

The sound-production organ within a bird is known as the syrinx. The syrinx is located between the air-sacs (or lungs) and the trachea, as can be seen in Figure 2.3.1, and is used in a similar way for the bird as the larynx is for humans. The anatomy of the syrinx can be seen in Figure 2.3.2. There has been debate as to whether the main sound generation

comes from the vibration of the drum head like medial tympaniform membrane(MTM) or the vibrating labia [1]. The model that will be used from [5] uses the latter theory, assuming the sound is generated by vibrations in the labia caused by pressure coming from the air-sacs.

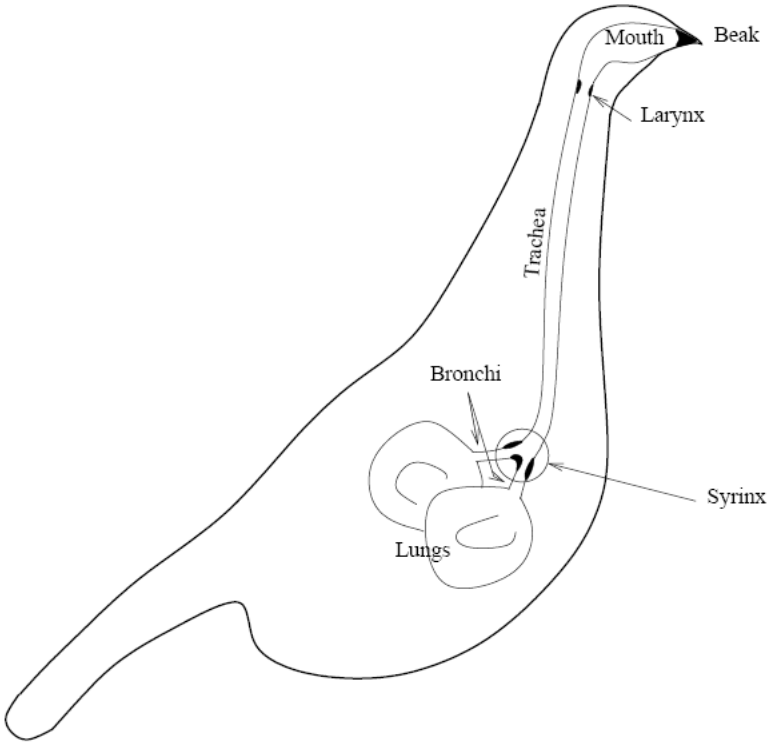

Figure 2.3.1. Location of the syrinx (image taken from [1])

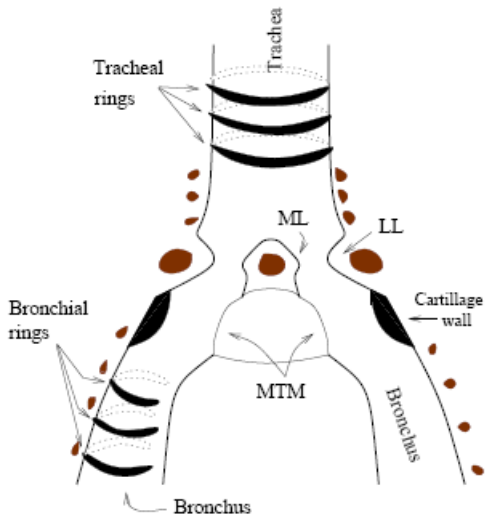

Figure 2.3.2. Anatomy of the syrinx (MTM) medial tympaniform membrane (ML) medial labia (LL) lateral labia (image taken from [1])

3
Recurrence Analysis

A large goal of the project was to determine if chaos was occurring in the Zebra Finch's song. Articles [9] and [8] are two examples of research focused on analysis of chaotic data related to bird vocalizations. In [9] Lyapunov exponents were used to classify chaotic bird calls, and in [8] Zebra-Finch syrinxes were found to be capable of producing highly nonlinear behavior. A first step toward determining if the Zebra Finch's song was chaotic was verifying that it was in fact deterministic. This was done by performing recurrence analysis on the birdsong data.

The techniques used for the recurrence analysis that will be discussed in this paper were primarily taken from frog calling research done through the University of Tokyo [11] [10]. These techniques are based around using recurrence plots (RP), **iso-directional recurrence plots** (IDRP) and **iso-directional neighbors plots** (IDNP) to determine if given data is deterministic or random. The university of Potsdam has put together a website [14] using research from [15] which is a great resource for understanding recurrence analysis.

3.1 Recurrence Plots

Definition 3.1.1. Let x_{t_n} be a time series and $\epsilon \in \mathbb{R}^+$. A **recurrence plot** for x_{t_n} is the set $\{(t_k,\ t_l) :\ |x_{t_k} - x_{t_l}| \leq \epsilon\}$.

Essentially a RP is a plot which illustrates the times when the given time series visits roughly the same value. Figure 3.1.1 illustrates how a general RP is made. The RP is a plot of the times (t_i) when the measured value was within a chosen threshold (ϵ) of itself. The value for ϵ is chosen so that 10% of the original data is plotted in the RP [11]. The points along the diagonal where $(t_i,\ t_i)$ is being plotted are disregarded when considering this 10% since they are meaningless and will always result in a point being represented in the RP. The points at t_1 and t_3 in the diagram are within ϵ of one another, so the times that the points occur are represented in the RP by plotting $(t_1,\ t_3)$ and $(t_3,\ t_1)$. Also note that the value of the time series data at time t_2 is not within the threshold ϵ of any other values, thus t_2 is not represented in the RP.

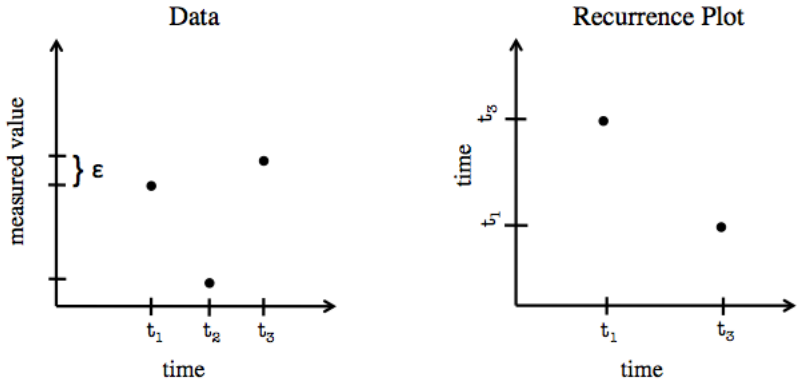

Figure 3.1.1. Recurrence plot construction

An example of an RP is given in Figure 3.1.3, where an RP has been constructed from the periodic time series data in Figure 3.1.2.

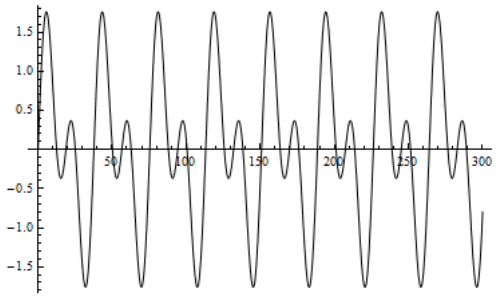

Figure 3.1.2. time series data from a periodic system

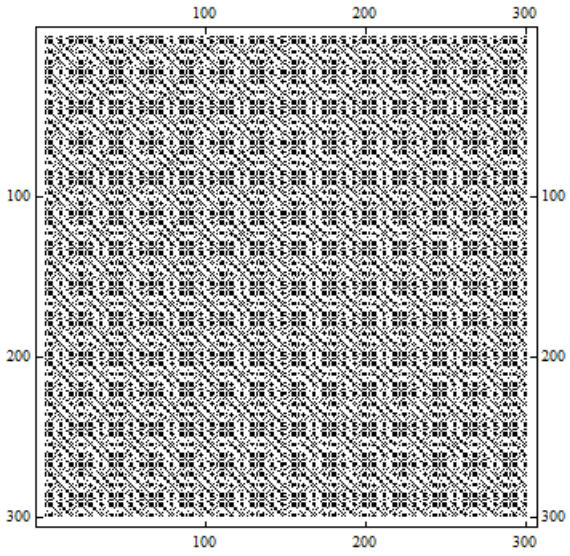

Figure 3.1.3. Recurrence plot of the time series data in Figure 3.1.2

Definition 3.1.2. Let x_{t_n} be a time series, $\delta \in \mathbb{R}^+$ and $d \in \mathbb{N}$. An **iso-directional recurrence plot** for x_{t_n} is the set $\{(t_k,\ t_l) :\ |(x_{t_k+d} - x_{t_k}) - (x_{t_l+d} - x_{t_l})| \leq \delta\}$.

An iso-directional recurrence plot is a plot which illustrates the times when the given time series data is heading roughly in the same direction. Figure 3.1.4 illustrates how a general IDRP is made. An IDRP is a plot of the times (t_i) when the changes in values to a future time $(t_i + d)$, which is a chosen number (d) of time steps away, are within δ of one another $(|\phi - \sigma| \leq \delta)$. As with the traditional RP's, the value for δ is chosen so that

10% of the original data (disregarding the diagonal) will be represented in the IDRP. The value for d is chosen so that the best results are achieved and can be found by trial and error. The value for d depends heavily on how high of a sample rate with which the data was collected.

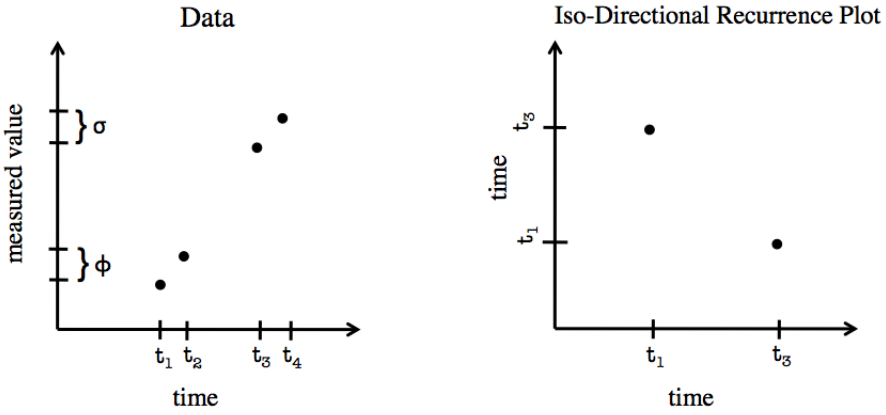

Figure 3.1.4. Iso-directional recurrence plot construction

An example of an IDRP is given in Figure 3.1.5, where an IDRP has been created from the time series data in Figure 3.1.2.

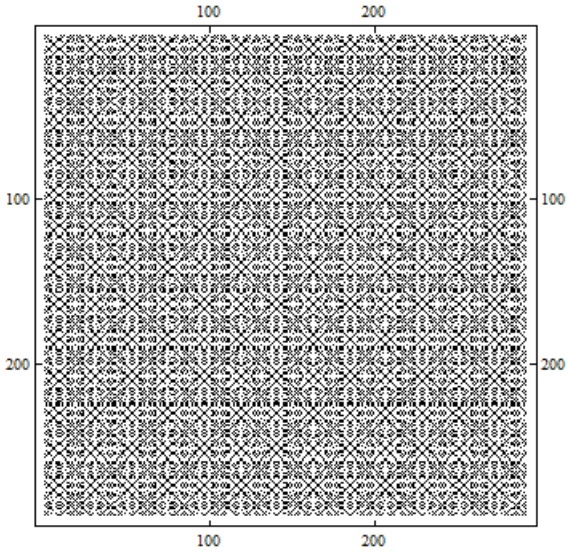

Figure 3.1.5. Iso-directional recurrence plot of the time series data in Figure 3.1.2

Definition 3.1.3. Let x_{t_n} be a time series. An **iso-directional neighbors plot** for x_{t_n} is the intersection of the recurrence plot and the iso-directional recurrence plot for x_{t_n}

An iso-directional neighbor plot illustrates when the given time series data is roughly the same value and is also roughly heading in the same direction. A general IDNP is made by plotting the intersection of the RP and the IDRP. An example of an IDNP is given in Figure 3.1.6, where an IDNP has been constructed from the time series data in Figure 3.1.2.

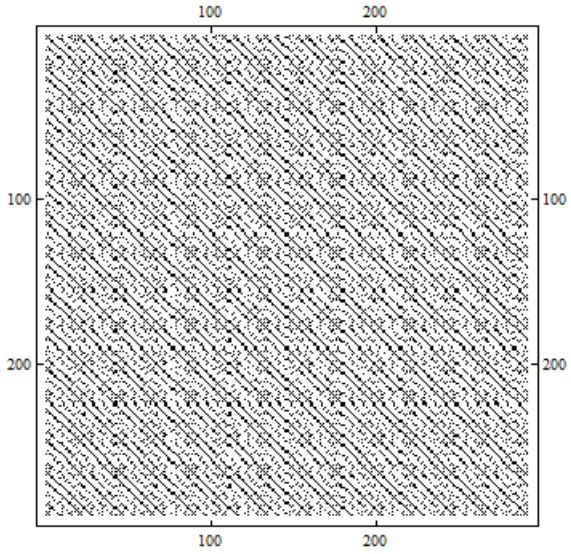

Figure 3.1.6. Iso-directional neighbor plot of the time series data in Figure 3.1.2

3.1.1 Recurrence Analysis and Determinism

As stated in Section 2.2, a fundamental feature of chaotic data is the fact that it is deterministic. A hallmark of deterministic data is the feature that if two points are at a similar value, they will be heading in a similar direction [11]. That is, if two points have similar values at times t_k and t_l, then the two points at some number of time steps d away t_{k+d} and t_{l+d} will have similar values as well.

If the data being analyzed is deterministic, and can be modeled by a low-dimensional dynamical system, then it must behave in a similar way to data that has come from a low-dimensional deterministic source. For instance, if the value 5 is input into a system, and the output is 10, then it is known that the system will always return 10 when 5 is input. If a value of 5.000000000001 is input into the same system, assuming this system to be low-dimensional, it would also be expected that a value somewhere near 10 would be output.

The three recurrence plots discussed in Section 3.1 are able to help determine if given time series data is deterministic or random. Figure 3.1.7 illustrates the ideal results for deterministic data. The times when the data points were near each other can be seen in the RP, and the times when the data points are heading in the same direction can be seen in the IDRP. Since these occur in the IDNP these are thus the same times, since the IDNP is the intersection of the RP and IDRP. This means that the points that are near one another are heading in the same direction. This example is of course an exaggeration to illustrate this technique for classifying deterministic data. The actual number of points present in the IDNP will be much lower than the number of data points present in the RP and IDRP. The percentage of points that is needed in the IDNP to classify the data as deterministic is discussed in Section 3.2. As can be seen in the example RP's given earlier, although the time series data exhibits very clear periodic deterministic behavior, the iso-directional neighbors plot is still shaded noticeably less than the other two RP's.

Figure 3.1.8 illustrates the ideal result for random data. The times when the data points were near each other can be seen in the RP, and the times when the data points are heading in the same direction can be seen in the IDRP. These are mostly *not* the same times since the IDNP is mostly empty. Because the data is being looked at on an interval, even random data will sometimes have points of similar value heading in the same direction. If the IDNP has been constructed from random data, however, the points should be more scattered

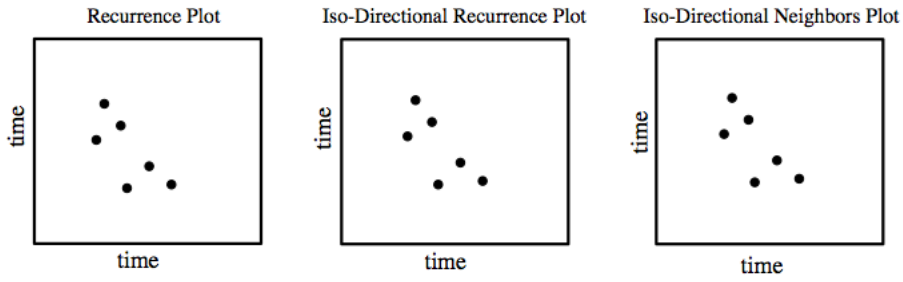

Figure 3.1.7. Recurrence analysis of deterministic data

and have less of a pattern than an IDNP constructed from deterministic data [10]. The percentage of points that is needed in the IDNP to classify the data as random will also be discussed in Section 3.2.

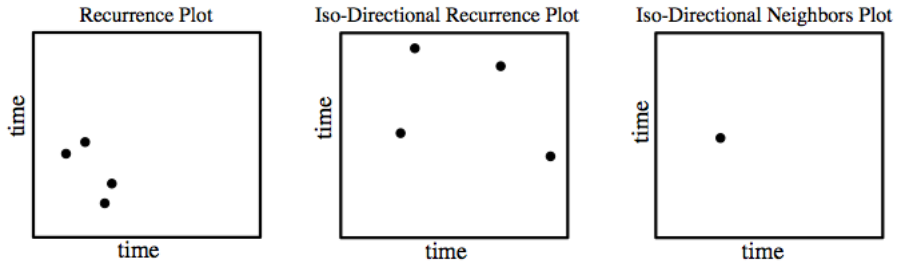

Figure 3.1.8. Recurrence analysis of random data

3.2 Recurrence Analysis Procedure

All of the recurrence analysis performed during this project was done within Mathematica. A Mathematica notebook was written for the three forms of recurrence plots discussed in Section 3 implementing techniques used in [11] and [10]. To determine the type of results that should be expected for chaotic data, recurrence analysis was performed on data output by a system which had already been classified as chaotic. The system chosen for this experiment was the system governed by the Hénon map. Recurrence analysis was then preformed on 1,600 points outputted by the Hénon map. Figure 3.2.1 shows the three

resulting RP's where $\epsilon = 0.2$, $\delta = 0.35$ and time steps $d = 3$. Thus the shading of these three recurrence plots are the ideal results for chaotic data.

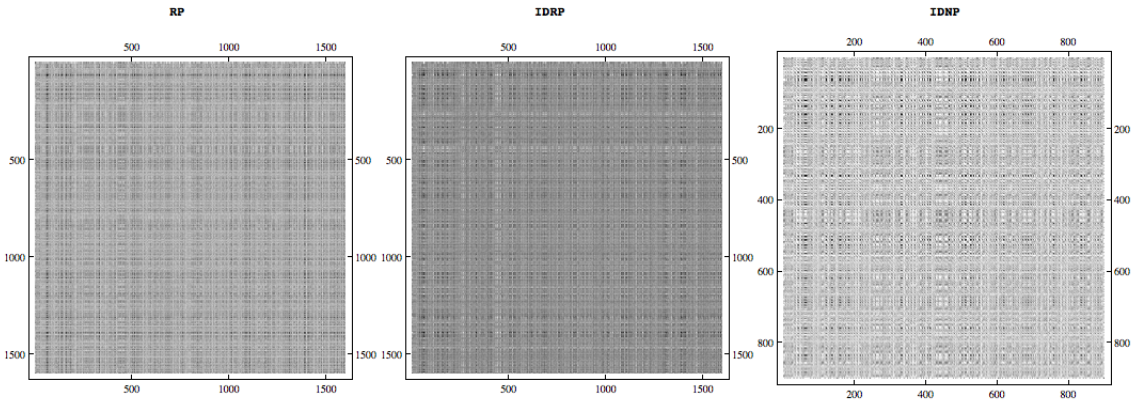

Figure 3.2.1. Recurrence analysis of the Hénon map with $\epsilon = 0.2$, $\delta = 0.35$ and $d = 3$

Recurrence analysis was also done to determine the expected results for random data. Recurrence analysis was performed on pseudo-random data which was obtained in Mathematica using the RandomReal command. The three resulting recurrence plots can be seen in Figure 3.2.2.

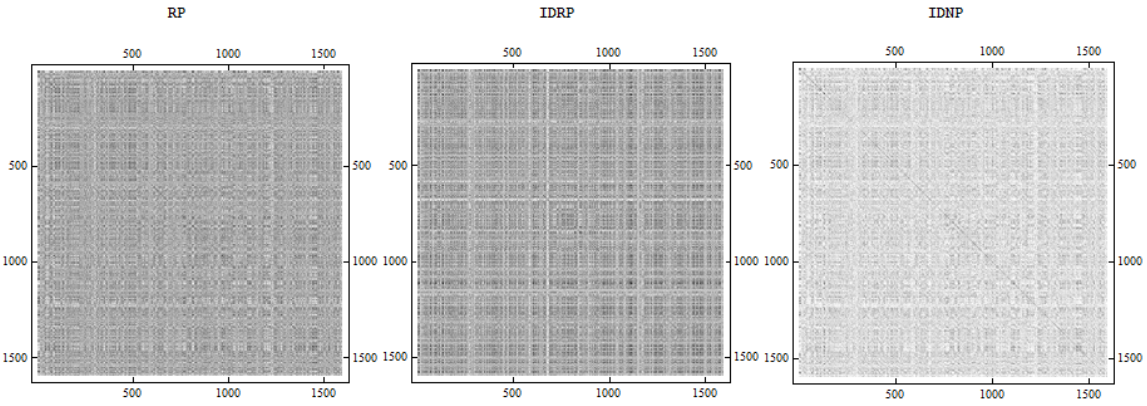

Figure 3.2.2. Recurrence analysis of pseudo-random data $\epsilon = 0.18$, $\delta = 0.25$ and d=3

The recurrence analysis discussed thus far has used the technique of creating the three recurrence plots directly from the time series data. As can be seen in [11] and [10] however, the recurrence plots can also be constructed from the delay plot (which will be

discussed in Section 4) of the time series data. This is a rather simple modification in the RP's construction process, where the relation between the vectors $(x_{t_k-j},\ x_{t_k-i},\ x_{t_k})$ and $(x_{t_l-j},\ x_{t_l-i},\ x_{t_l})$ with delay parameters i and j is investigated instead of the relation between the points x_{t_k} and x_{t_l}. The three RP's were made of Hénon map and the pseudo-random data using this delay plot construction technique. Figure 3.2.3 is the resulting recurrence plots of the Hénon map with delay parameters $j = 2$, $i = 1$ thresholds $\epsilon = 0.588$, $\delta = 1.093$ and time steps $d = 3$, and Figure 3.2.4 is one example of the pseudo-random RP's that were made with delay parameters $j = 2$, $i = 1$ thresholds $\epsilon = 0.55$, $\delta = 0.73$ and time steps $d = 3$.

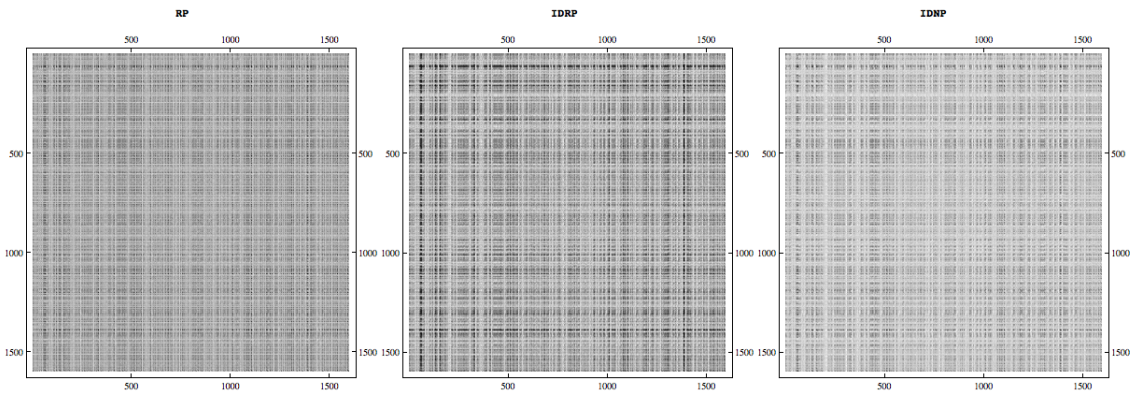

Figure 3.2.3. Recurrence plots constructed from delay plots of Hénon map with $\epsilon = .588$, $\delta = 1.093$ and d=3

It became clear from these plots that the graphical representation of the RP's might not offer enough information to come to a clear conclusion on whether to classify the data as deterministic or random. Mostly due to image size and resolution issues, it was too difficult to tell the difference between the two data types. The results were better when the recurrence plots were viewed with image sizes closer to a pixel per point; they were, however, still not precise enough. Figure 3.2.5 and Figure 3.2.6 illustrate this point. Figure 3.2.5 is the top left sections of the RP and IDNP of the Hénon map shown in

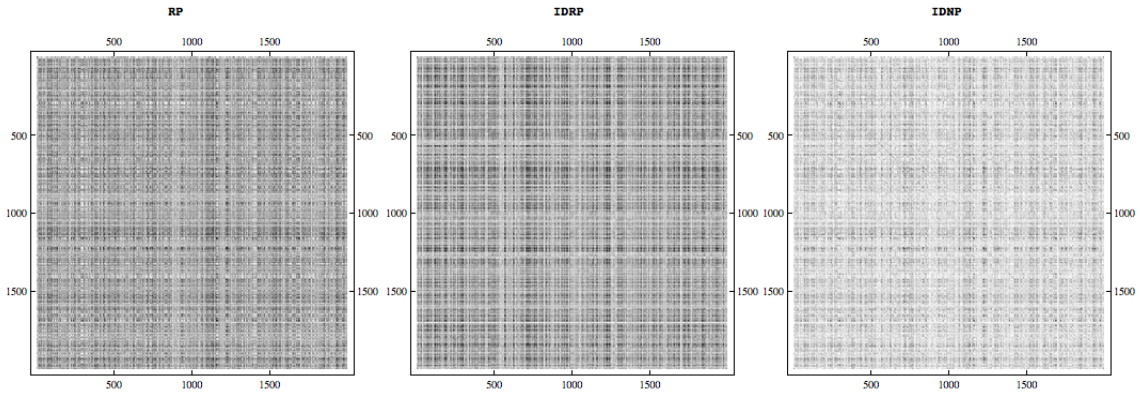

Figure 3.2.4. Recurrence plots constructed from delay plots of pseudo-random data with $\epsilon = 0.18$, $\delta = 0.25$ and d=3

Figure 3.2.1 viewed at four times the size. Figure 3.2.6 is the top left sections of the RP and IDNP of pseudo-random data shown in Figure 3.2.2 viewed at four times the size.

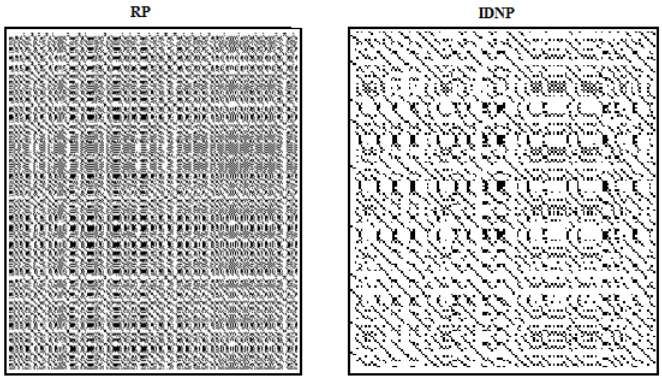

Figure 3.2.5. The top left sections of the RP and IDNP in Figure 3.2.1

Along with the obvious lighter shading of the pseudo-random data's IDNP from that of the Hénon's IDNP, as expected there also seems to be less order among the points present. However, because of the inconsistencies that arise with real-world data that will be present in the birdsong recordings, the difference between the two data sets' IDNP's did not seem large enough.

To combat this problem the correlation between the RP and the IDRP was computed. The correlation of the Hénon map's RP and IDRP (using the same parameters that were

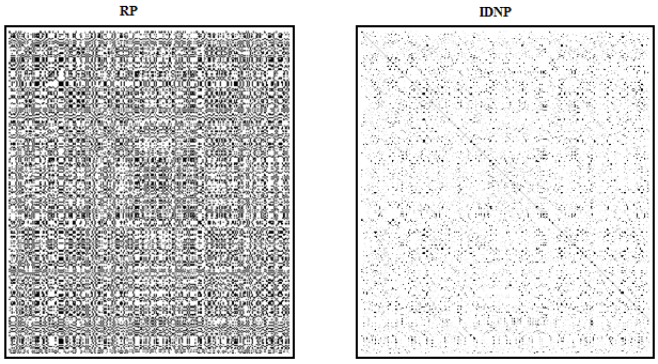

Figure 3.2.6. The top left sections of the RP and IDNP in Figure 3.2.2

used in the previous examples) constructed directly from the time series data was 0.34, while the correlation of the Hénon map's RP and IDRP constructed from delay plots was found to be 0.55.

As stated in section 3.1.1, because the data in the RP and IDRP are within an interval, there should be at least a small correlation between the two for random data. To get an idea of what the correlation between the RP and IDRP should be for random data, 20 trials were run using pseudo-random data. This process was done for both the RP's constructed directly from the time series data and those constructed from the delay plots.

From these trials it was determined that the standard deviation of the correlations between the RP and the IDRP constructed from the delay plots was 0.0086 with a maximum correlation value of 0.34 and a minimum of 0.298. The standard deviation of the correlations between the RP and IDRP constructed from the time series data was 0.0075 with a maximum correlation of 0.17 and a minimum correlation of 0.143. From these values it can easily be calculated when the RP and the IDRP were constructed from the delay plot, the correlation between the Hénon map's RP and IDRP was approximately 14 standard deviations greater than the max pseudo-random data's correlation. When the RP and IDRP was constructed directly from the time series data, the correlation between the Hénon map's RP and IDRP was approximately 23 standard deviations greater than

the max pseudo-random data's correlation. Both results seem to show a clear difference between random and deterministic data. Based on this result it was chosen to perform the recurrence analysis on the birdsong data using the RP's constructed directly from the time series data.

3.3 Recurrence Analysis Results

Several aperiodic sections of birdsong data tested returned correlation values between the RP and IDRP greater than 0.2. A 300 point sample of the time series data from an example of one of these sections of aperiodic birdsong can be seen in Figure 3.3.1. Figure 3.3.2 is the recurrence analysis of this birdsong section. The plot is made from 968 data points with thresholds $\epsilon = 0.2$, $\delta = 0.33$ and the number of time steps $d = 3$. The darker appearance of the recurrence plots compared to the previous examples is due to the sharper contrast which is due to the fact that fewer points are being analyzed. The correlation value between the RP and IDRP of this particular section of song was 0.36, which is approximately 25 standard deviations away from the maximum pseudo-random correlation found. This result clearly suggests this section of birdsong is deterministic.

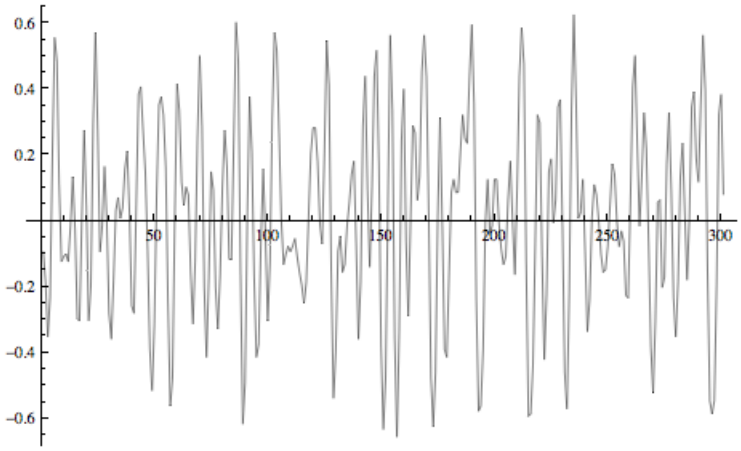

Figure 3.3.1. Time series of an aperiodic birdsong section

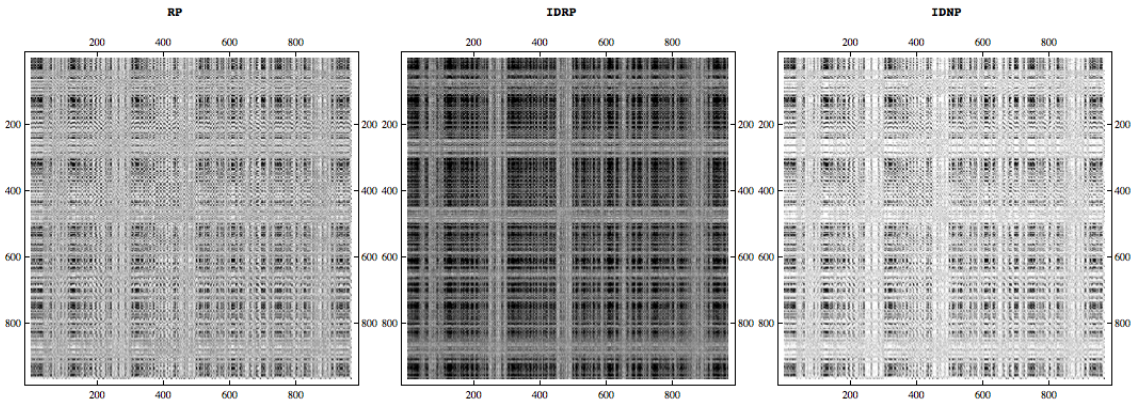

Figure 3.3.2. Recurrence Analysis of an Aperiodic Birdsong Section with $\epsilon = 0.2$, $\delta = 0.33$ and $d = 3$

4
Delay Plot Analysis

Having successfully classified aperiodic sections of Zebra Finch song as deterministic, this data was now analyzed for chaos. Delay plots were used to determine if the birdsong data displayed evidence of coming from a chaotic system by reconstructing the state space. As stated in Section 2.1 if the data had come from a chaotic system the state space should contain a strange attractor. In [9] Fletcher uses delay plots, his results proved to be inconclusive however, and he suggests the main cause of this may have been due to interference from background sounds in the in-vivo recordings he used. The data obtained for this project in comparison came from recordings performed in a laboratory and exhibited minimal background noise.

4.1 Delay Plots

The techniques used for creating the delay plots in this paper were taken from [12] and [11]. As with the recurrence plots another resource utilized was [14] which was based heavily around research done for [15]. Delay plots can be a very useful tool when analyzing chaotic data, especially when determining if aperiodic time series data is random, periodic

or chaotic. They can be used to reconstruct trajectories in the state space, and in doing so can reconstruct the strange attractor a chaotic system creates in the state space. Which is remarkable when considering a delay plot is only utilizing one variable from the system which produced the time series.

A delay plot can be constructed from time series data by taking the point x which occurs at time t denoted x_t, and plotting the three dimensional vector $(x_{t-j},\ x_{t-i},\ x_t)$. This technique is commonly referred to as **time delay embedding**, where $i,\ j$ are known as the **delay parameters** [14]. The delay parameters $i,\ j$ are the amount of time being subtracted from the time t that the original point occurred. Thus with discrete data, $i,\ j,\ t$ will be natural numbers. A schematic diagram of the construction of a delay plot can be seen in Figure 4.1.1. Where $\beta,\ \delta$ and ϕ are the respective values of time series data at times $(t-j)$, $(t-i)$ and (t).

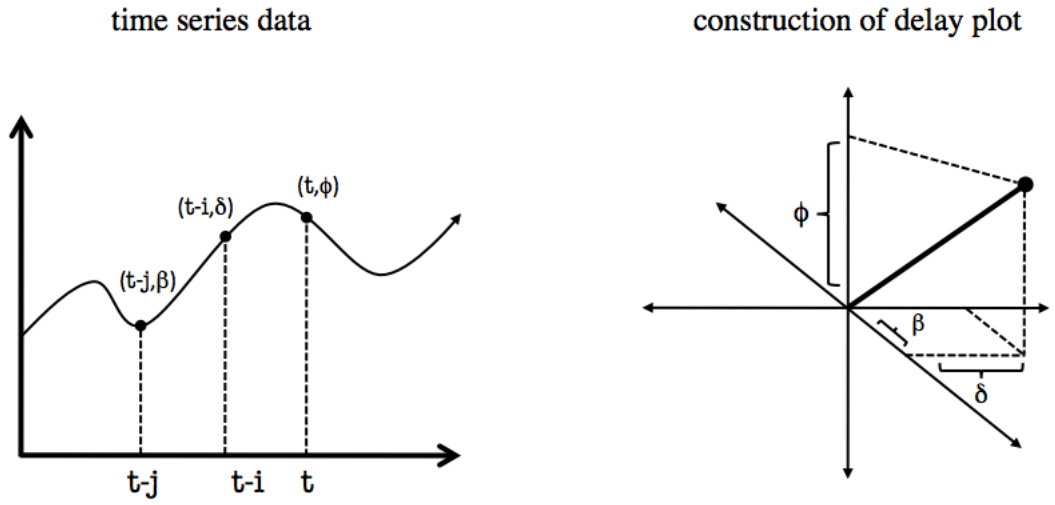

Figure 4.1.1. Constructing a delay plot from time series with delay parameters i, j

As discussed in Section 2.2 chaotic systems have strange attractors in their state space. The purpose of a delay plot is to visually detect the existence of the "order" that is caused by this attractor. If the time series data being analyzed is from a low-dimensional

(preferable three-dimensions or lower) chaotic source, it is expected there will be evidence of the attractor "order" represented in the delay plot. On the other hand if the time series arises from a stochastic source, it is expected there will be no evidence of this order [12]. If the given time series data is periodic, the delay plot will be some set of closed curves. An example of this can be seen in Figure 4.1.2, where a delay plot can be seen along with the periodic time series it was constructed from. Figure 4.1.3 shows time series data from a periodic system with a more complex period and the resulting delay plot. Notice the delay plots complexity has also increased while still maintaining the closed looped structure of a periodic delay plot. It is very important when using delay plot analysis to choose the right

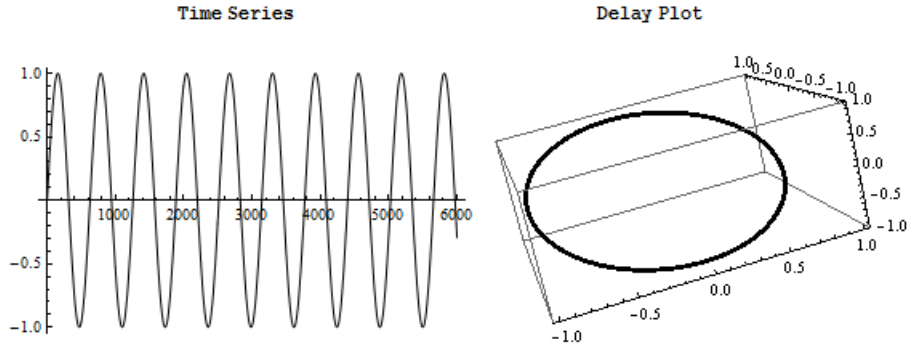

Figure 4.1.2. Delay plot constructed from simple periodic time series data

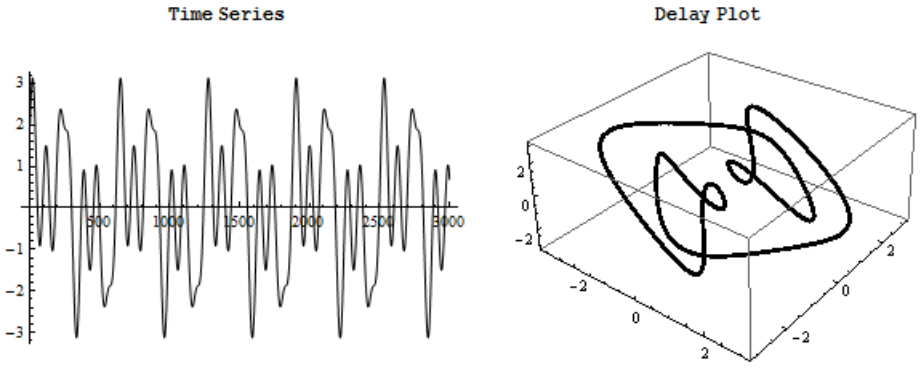

Figure 4.1.3. Delay plot constructed from complex periodic time series data

delay parameters. If the delay parameters are too small, too big or too far away from one

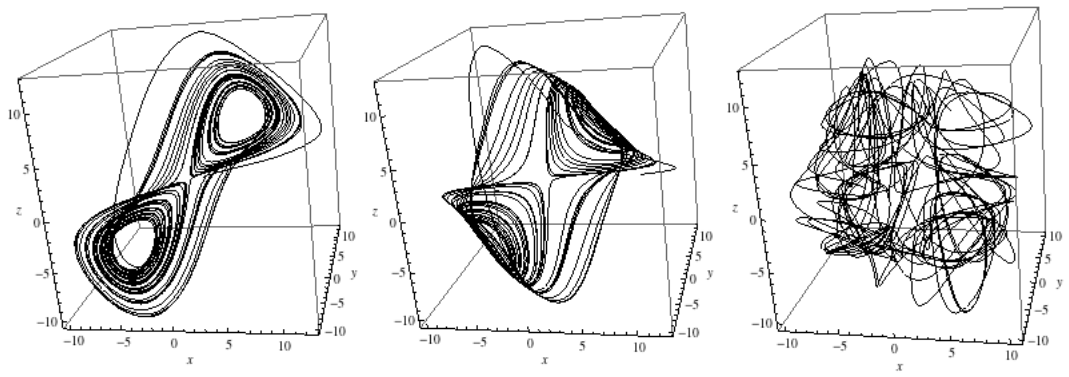

Figure 4.1.4. Delay plot of lorenz oscillator left plot $j = 3, i = 1$ middle plot $j = 6, i = 3$ right plot $j = 51, i = 17$

another, this can create problems when it comes to the visual detection of "order". The most serous of these problems can be an almost complete loss of this "order" in the delay plot. On the less problematic side of the spectrum there could also be a certain amount of squashing or stretching that occurs to the reconstruction of the attractor. The method chosen to combat this problem when choosing the delay parameters was that of trial and error.

Figure 4.1.4 illustrates the importance of choosing good delay parameters. The three delay plots are all constructed from 1000 points of a solution to one of the three differential equations from the Lorenz oscillator. The plot on the left which clearly exhibits characteristics of the Lorenz attractor which can be seen in Section 2.2.3, was constructed with delay parameters $j = 3,\ i = 1$. The plot in the middle which is a more squished version of the Lorenz attractor has delay parameters $j = 6,\ i = 3$ and the plot on the right which has almost entirely lost the evidence of an attractor has embedding parameters $j = 51,\ i = 17$.

4.2 Delay Plot Analysis Procedure

All of the analysis performed using delay plots during this project was done within Mathematica. A Mathematica notebook was written for the delay plots as discussed in Section 4.1

mainly implementing techniques used in [11] and [12]. To determine the type of results that should be expected for chaotic data, delay plots were made from data output by two systems which had already been classified as chaotic. As in Section 3.2 the first system chosen was the system governed by the Hénon map. A delay plot was then made with delay parameters $j = 2$, $i = 1$ from 1,600 points outputted by the Hénon map. Figure 4.2.1 shows a sample 100 data points of the time series data omitted by the Hénon map and the resulting delay plot which exhibits an obvious non-scattered geometry.

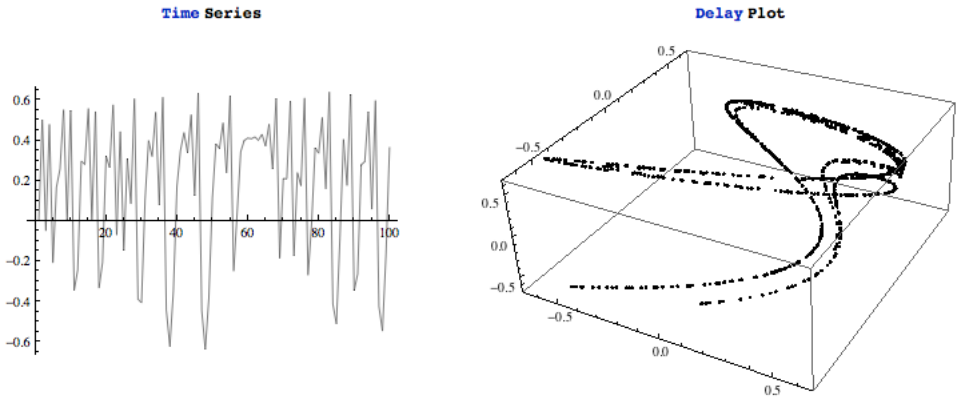

Figure 4.2.1. Sample of the Hénon map's time series and delay plot with j=2,i=1

A delay plot was also constructed from one of the differential equations governing the Lorenz Oscillator. Figure 4.2.2 shows the time series data of the solution $x(t)$ for the Lorenz Oscillator evaluated to $t = 200$ and the corresponding delay plot that was created from this data. A sample rate of 0.001 was used when selecting points, so the delay parameters were much larger than the previous example with $j = 300$ and $i = 220$.

Delay plots were also made to determine the expected results for random data. Delay plots were made using pseudo-random data which was obtained in Mathematica using the RandomReal command. An example of these delay plots can be seen in Figure 4.2.3, with a sample 100 points of the time series data on the left and the delay plot on the right. As was expected there is a noticeable scattered lack of order to the delay plot. Several

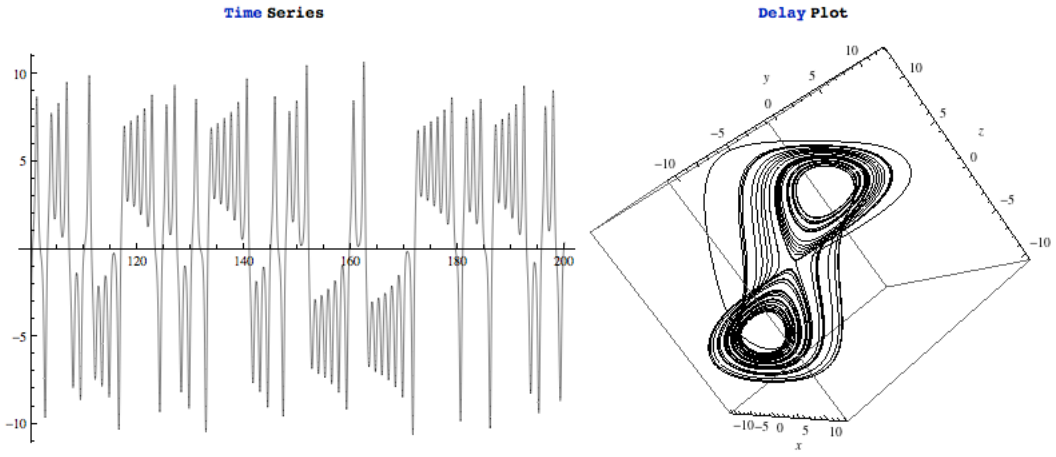

Figure 4.2.2. Time series and delay plot of the lorenz oscillator's solution $x(t)$ with delay parameters $j = 300$ and $i = 220$

different sets of delay parameters were tested and all returned similar orderless results. It is quite remarkable how clear a difference there is between the pseudo-random delay plot and the Hénon delay plot, while the time series data of the two data sets seems fairly similar.

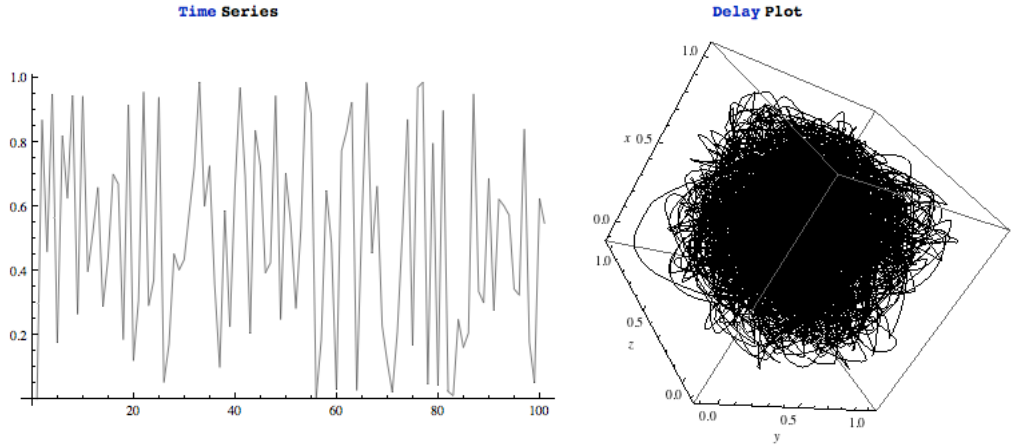

Figure 4.2.3. Sample of pseudo-random time series and delay plot with j=2,i=1

To get a better understanding of what the birdsong delay plots should look like, a delay plot was constructed from a periodic section of birdsong. A section of birdsong was selected which clearly exhibited periodic behavior and had a fairly small number of frequencies.

Figure 4.2.4 shows a 400 point sample of the periodic birdsong's time series, and the resulting delay plot. The delay plot was constructed from 800 points of the time series data, with j=4 and i=2.

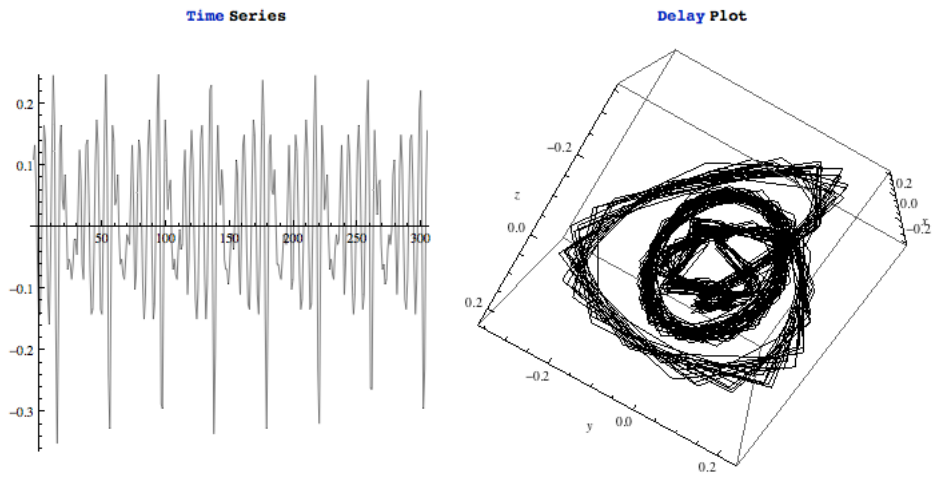

Figure 4.2.4. Sample of periodic birdsong time series and delay plot with j=4,i=2

It became clear from this plot that the sample rate of the recording was not high enough to produce good delay plots. To solve this dilemma interpolation was performed on the birdsong data. The interpolation was done using Mathematica's ListInterpolation command. The resulting delay plot can be seen in Figure 4.2.5.

Delay plots were then made from the aperiodic sections of birdsong which had been classified as deterministic using recurrence analysis in Section 3.2. An example of one of these delay plots can be seen in Figure 4.2.6.

It is somewhat difficult to see from the two-dimensional version in Figure 4.2.6, but the general form exhibited by most of the birdsong delay plots was that of a somewhat squished sphere possibly displaying a tube running through the middle. Since the data had already been classified as deterministic there could be two possibilities for what type of data would form such a delay plot. The data could be a higher dimensional chaotic system than the two chaotic examples discussed, where the attractor was a three dimensional

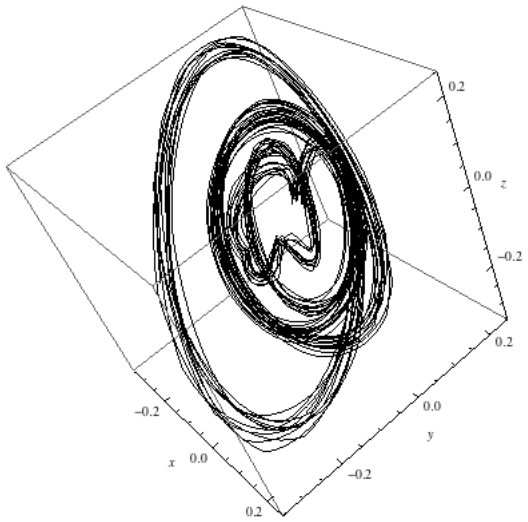

Figure 4.2.5. Periodic birdsong delay plot from interpolated data with j=4,i=2

surface such as a torus. Otherwise the data could be periodic data with enough noise added in to give the data the effect of being aperiodic but not enough so that it failed the recurrence analysis determinism test.

To test the theory that the data was coming from a higher dimensional chaotic source, and the delay plot was showing evidence of a three dimensional attractor, the delay plot was cut up into slices. This was done in a way as if an MRI was being taken of the delay plot, with the hope being these slices would offer more insight into whether or not there was an actual tube running through the center of the delay plot. Figure 4.2.7 shows six slices of the delay plot in Figure 4.2.6, with the first slice being in the top left corner and the last slice in the bottom right.

The results from this slicing seemed to suggest the delay plots were in fact not torus-like, and may be exhibiting more of a tangle of curves in the center of the sphere of curves, which is more characteristic of periodic data.

To test the theory that these delay plots were actually being made from periodic data mixed with noise, actual periodic data mixed with noise would have to be found that

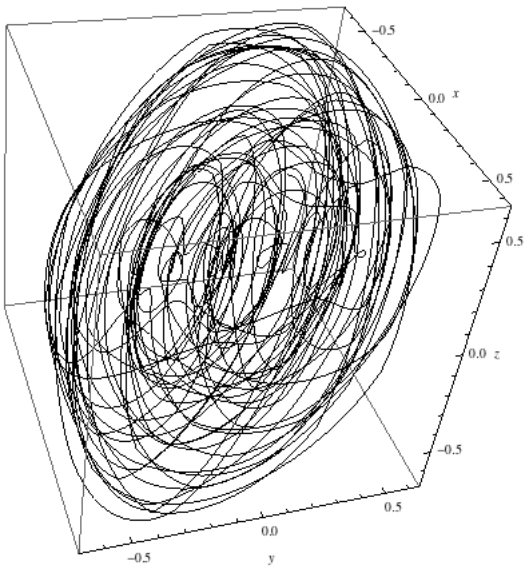

Figure 4.2.6. Delay plot of a section of deterministic aperiodic birdsong

could create similar delay plots. To help make this data, histograms of the frequencies present in the birdsong data were made. An example of one of these histograms can be seen in Figure 4.2.8, where the histogram has been created from the birdsong data which the delay plot was constructed from in Figure 4.2.6.

The most predominant frequencies present in the histogram were then identified. A function was then defined in Mathematica made up of a sum of sine functions with the frequencies taken from the histogram. These sine functions were also weighted depending on how predominant their frequency was in the histogram. Equation 4.2.1 is a function that was constructed from a histogram of a birdsong.

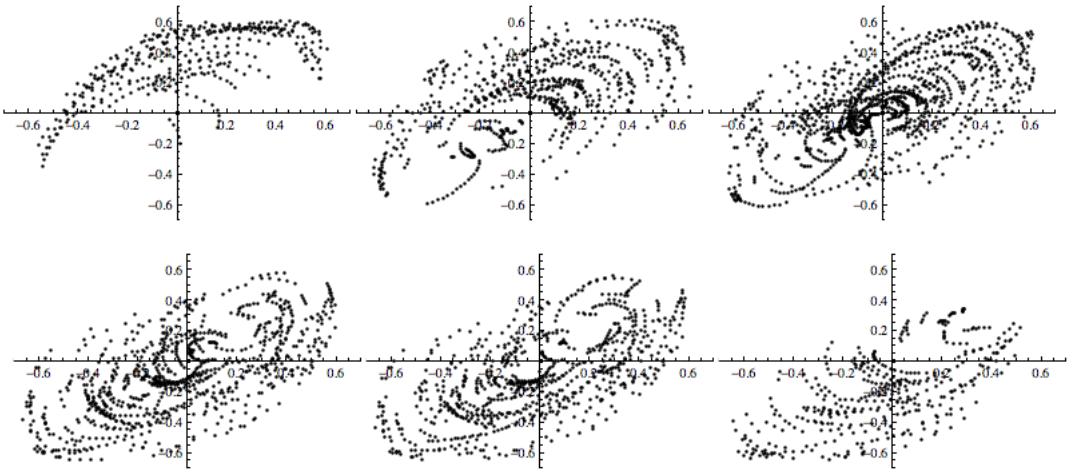

Figure 4.2.7. Slices of deterministic aperiodic birdsong delay plot

$$
\begin{aligned}
\text{f(x)}= &\sin(0.491736x) + 3\sin(0.495868x) + 3\sin(0.496901x) + 2\sin(0.497934x)\\
&+\sin(0.498967x) + 2\sin(0.506198x) + 3\sin(0.507231x) + 3\sin(0.508264x)\\
&+3\sin(0.509298x) + 3\sin(0.510331x) + 2\sin(0.511364x) + \sin(0.524793x)\\
&+\sin(0.530992x) + \sin(0.532025x) + \sin(0.533058x) + \sin(0.534091x)\\
&+\sin(0.615702x) + \sin(0.709711x) + \sin(0.713843x) + 2\sin(0.732438x)\\
&+2\sin(0.733471x) + \sin(0.789256x) + \sin(0.790289x) + \sin(0.83781x)\\
&+\sin(0.838843x) + \sin(0.842975x) + \sin(0.844008x) + 2\sin(0.899793x)\\
&+2\sin(0.900826x) + 2\sin(0.916322x) + 2\sin(0.917355x) + \sin(0.927686x)\\
&+\sin(0.928719x) + \sin(1.1219x) + \sin(1.12293x) + \sin(1.12397x)\\
&+3\sin(1.12913x) + 3\sin(1.13017x) + 3\sin(1.1312x) + 2\sin(1.1405x)\\
&+3\sin(1.14153x) + 3\sin(1.14256x) + 2\sin(1.1436x) + \sin(1.14463x)\\
&+\sin(1.15599x) + \sin(1.15909x) + 2\sin(1.16012x) + 2\sin(1.16426x)\\
&+2\sin(1.16529x) + \sin(1.16632x) + \sin(1.17355x) + 2\sin(1.17459x)\\
&+3\sin(1.18079x) + 3\sin(1.18182x) + 3\sin(1.18285x) + 3\sin(1.18388x)\\
&+2\sin(1.20145x) + 3\sin(1.20248x) + 3\sin(1.20351x) + 3\sin(1.20661x)\\
&+3\sin(1.20764x) + 2\sin(1.21074x) + 3\sin(1.21178x) + 3\sin(1.22211x)\\
&+3\sin(1.22314x) + \sin(1.22417x) + 2\sin(1.22727x) + \sin(1.22831x)\\
&+\sin(1.23244x) + \sin(1.23347x) + \sin(1.24174x) + \sin(1.24587x)\\
&+\sin(1.2469x)
\end{aligned}
\tag{4.2.1}
$$

A sufficient amount of noise was then added to this function's output using Mathematica's RandomReal command until its spectrogram closely resembled the birdsong data's spectrogram. Figure 4.2.9 shows the two spectrograms, with the birdsongs on top and the functions on the bottom. Figure 4.2.10 shows the time series data of the two data

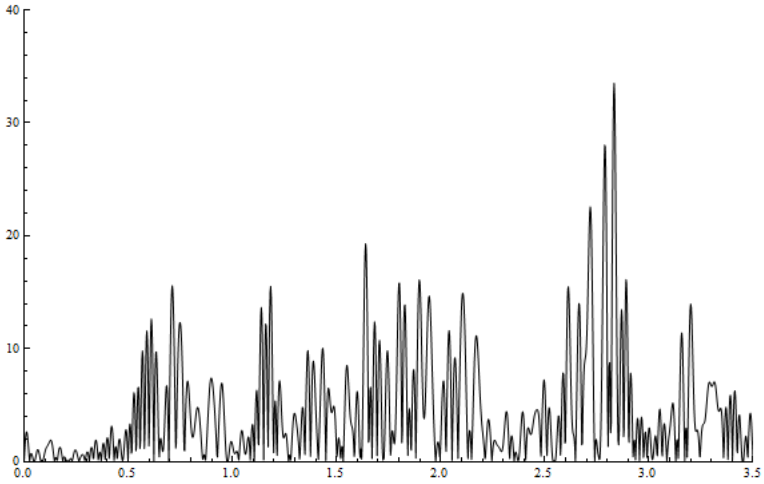

Figure 4.2.8. Histogram of the different levels of frequencies present in birdsong

sets, which also share a somewhat similar structure. As a last test of the two data sets'

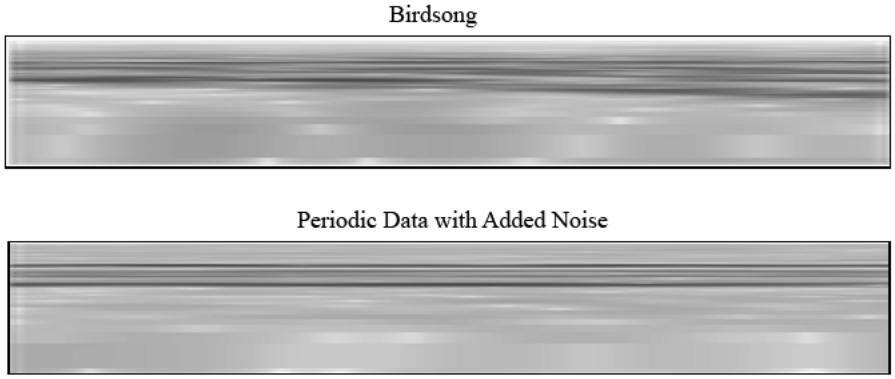

Figure 4.2.9. Birdsong spectrogram (seen top) and periodic data with noise added in (bottom)

similarity, recurrence analysis was performed on the periodic data with added noise. The data generated from Equation 4.2.1 returned a correlation value between its RP and IDRP of 0.38, 28 standard deviations from the highest random data's correlation: clearly high enough to classify the data as deterministic.

After the recurrence analysis, delay plots were finally made of the data sets generated from the periodic functions output with added noise. Figure 4.2.11 shows the resulting

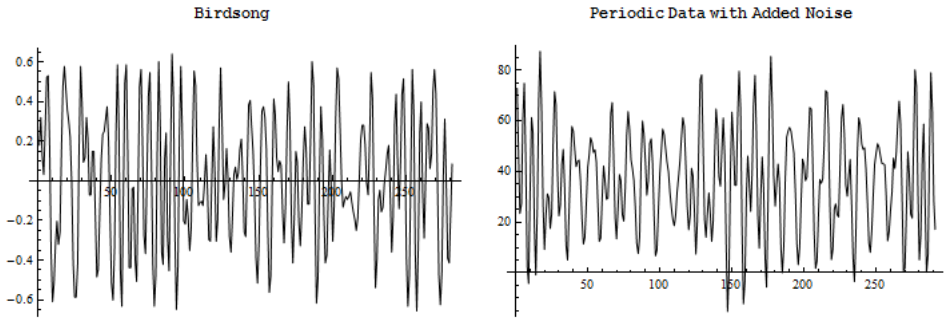

Figure 4.2.10. Birdsong time series (right) and periodic data with added noise (left)

delay plot. It can be somewhat difficult to see from the two-dimensional version of the delay plot, but the delay plot in Figure 4.2.11 has a strikingly similar structure to that of the delay plot constructed from the birdsong data in Figure 4.2.6.

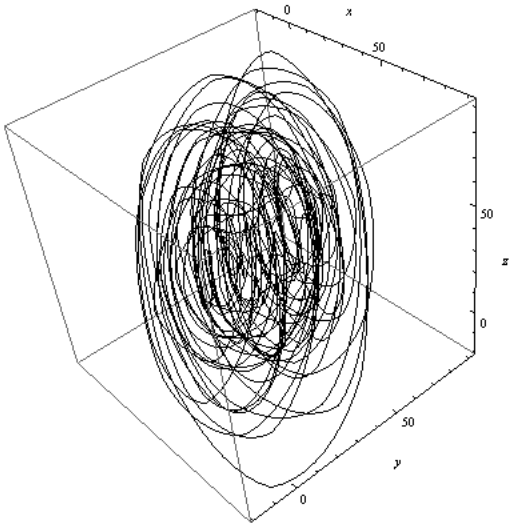

Figure 4.2.11. Delay plot of periodic data with added noise

4.2.1 Results of Delay Plot Analysis

Based on the results from Section 4.2, it seems likely that the aperiodic sections of the Zebra Finch calls analyzed were *not* chaotic. Because of the similarity between the delay

plots of the birdsong and the periodic data with added noise, it seems likely that the birdsong data is in fact periodic with added noise.

Looking back, the recurrence analysis may also have hinted at this result. Where as the IDNP of the system governed by the Hénon map was much more consistently shaded, the birdsong's IDNP has a much larger contrast in its shading even when being viewed at an appropriate image size. The reason for this could be due to the fact that the Hénon map is deterministic whereas the birdsong only has small sections which display deterministic behavior.

The other possibility for the lack of a clear chaotic attractor could be the same problem as suggested in [9], which is that the birdsong data was not stationary. Because of the remarkably quick ability of the Zebra Finch to change tones, it is hard to rule this possibility out. A final possibility is that the system generating the data may be of too high a dimension for the delay plot to properly reconstruct the state space.

5
Analysis of Syrinx Models

As was discussed in Section 3.2, there has been clear evidence of chaos in bird vocalization-related data. In [9] Fletcher classified sections of two different bird calls (that of the Sulfur Crested Cockatoo and the Gang-gang Cockatoo) as chaotic. In [8] Fee *et al.* found evidence of period doubling working with an isolated Zebra Finch Syrinx. Because of this, it was an important aim of the project to find evidence of chaos in models of the syrinx as an attempt to verify that the model was capable of producing even the most complex of bird vocalizations.

Although there has been a long standing debate as to whether the main sound generation in the syrinx comes from the vibration of the MTM or the labia, recent studies have provided substantial evidence for the latter theory [1]. In [8] Fee *et al.* showed a Zebra Finch syrinx was capable of producing a large array of sounds even after the removal of the MTM. Because of this the model that was chosen uses the theory of the sound production coming from the labia. The model, taken from [5] is an extension of a well known two-mass model of the human vocal-folds.

5.1 Modeling the Syrinx

There has been a substantial amount of work done in the field of human vocal-fold modeling. One of the most well known models for the human vocal folds is Ishizaka & Flanagan's two-mass model [3]. The general idea behind the two-mass model is to model the human vocal fold as two coupled harmonic oscillators. In [4] Steineche & Herzel found bifurcations in a simplified asymmetric version of the model, meaning the two sets of masses were not moving in unison. The symmetric form of the model from [4] is given in Equations 5.1.1-5.1.8, and a schematic diagram of the model can be seen in Figure 5.1.1.

$$\dot{x}_1 = v_1 \tag{5.1.1}$$

$$\dot{v}_1 = \frac{1}{m_1}\Big(P_1 l d_1 - r_1 v_1 - k_1 x_1 - \Phi(-a_1) c_1 \frac{a_1}{2l} - k_c(x_1 - x_2)\Big) \tag{5.1.2}$$

$$\dot{x}_2 = v_2 \tag{5.1.3}$$

$$\dot{v}_2 = \frac{1}{m_2}\Big(P_2 - r_2 v_2 - k_2 x_2 - \Phi(-a_2) c_2 \frac{a_2}{2l} - k_c(x_2 - x_1)\Big) \tag{5.1.4}$$

The subscripts 1,2 represent which mass the parameter is associated with, 1 being the lower mass and 2 being the upper mass. The variables $a_1 = a_{01} + 2lx_1$ and $a_2 = a_{02} + 2lx_2$ are the lower and upper glottal areas. The rest of the parameters are defined as follows:

- l is the length of the trachea
- d_i is the height of the respective mass
- r_i is a damping constant of the respective mass
- k_i is the spring constant of the respective mass
- k_c is the coupling constant between the upper and lower masses
- c_i represents an additional spring constant which arises during a collision between the right and left masses

- $\Phi(x)$ describes this collision
- x_i represents the distance the mass is from the mid line
- m_i is the respective mass
- P_i is the pressure inside the glottis acting on mass i and is given by Equations 5.1.6 and 5.1.7.

$$a_{\min} = \begin{cases} a_1, & \text{if } 0 < x_1 < x_2 \\ a_2, & \text{if } 0 < x_2 \leq x_1 \\ 0, & \text{otherwise} \end{cases} \tag{5.1.5}$$

$$P_1 = P_s\Big(1 - \Phi(-a_{\min})\Big(\frac{a_{\min}}{a_1}\Big)^2\Big)\Phi(a_1) \tag{5.1.6}$$

$$P_2 = 0 \tag{5.1.7}$$

Note that by defining P_2 in this way, the assumption is being made that the subglottal pressure P_s is only having an effect upon P_1.

$$\Phi(x) = \begin{cases} \tanh(50x/a_0), & \text{if } x > 0 \\ 0, & \text{if } x \leq 0 \end{cases} \tag{5.1.8}$$

In the case of $\Phi(a_{\min})$ an implicit Φ function is defined where $a_{\min} = \max(0,\ a_{\min})$. The parameters for the symmetric version of the model given in [4] are as follows: $m_1 = 0.125$, $m_2 = 0.025$, $r_1 = r_2 = 0.02$, $k_1 = 0.08$, $k_2 = 0.008$, $k_c = 0.025$, $c_1 = 3k_1$, $c_2 = 3k_2$, $d_1 = 0.25$, $d_2 = 0.05$, $a_{01} = a_{02} = 0.05$, $P_s = 0.008$. All of the units are given in centimeters, grams, milliseconds and their equivalent combinations.

The asymmetric version of this model involves changing the parameters between the two sets of masses. It also has added terms which effect the k's, c's and m's to simulate vocal fold paralysis disorders.

In [6] using the Steineche & Herzel model with

$$a_{\min} = \begin{cases} a_1, & \text{if } 0 < x_1 < x_2 \\ a_2, & \text{if } 0 < x_2 \leq x_1 \end{cases}$$

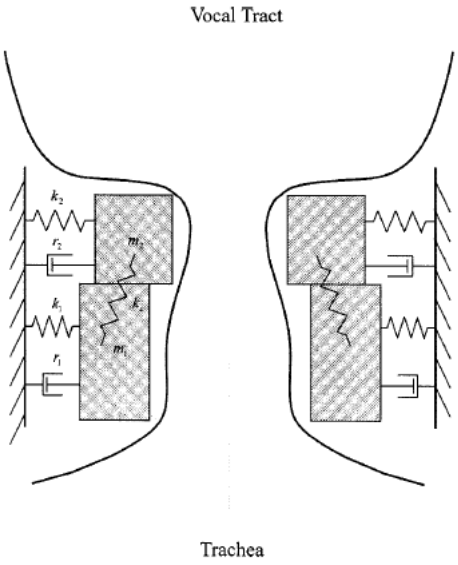

Figure 5.1.1. Schematic diagram of the symmetric two-mass model (image taken from [6])

disregarding the change to $a_{\min}$ in the case of $\phi(a_{\min})$ and a few parameter changes ($r_1 = 0.01$, $P_s = 0.05$ and $k_c = 0.09$, $x_1(0) = x_2(0) = 0.1$,$v_1(0) = v_2(0) = 0.0$), Jiang *et al.* were able to find chaotic solutions for the differential equations governing the system.

In [5] Herzel *et al.* adapt the Steineche & Herzel model to a song bird syrinx. The model of the syrinx is simply a scaling down of the symmetric version of the vocal fold model, with the default parameters as follow: $l = 0.3$, $a_{01} = 0.0021$, $a_{02} = 0.00175$, $d_1 = 0.1$, $d_2 = 0.02$, $m_1 = 0.0015$, $m_2 = 0.0003$, $k_1 = 0.08$, $k_2 = 0.008$, $r_1 = r_2 = 0.002$, $k_c = 0.0025$, $c_1 = 3k_1$, $c_2 = 3k_2$.

5.2 Testing Human Vocal Folds Model

To get a better idea of how two-mass models work and what their delay plots would look like, the human version of the two-mass model was analyzed for chaos. The symmetric vocal fold model from [6], discussed in Section 5.1, was implemented in Mathematica. The model was then evaluated for the chaotic parameters given in [6], and a delay plot was

made from the results. Figure 5.2.1 shows the chaotic time series of the solution $x(t)$ and the resulting delay plot.

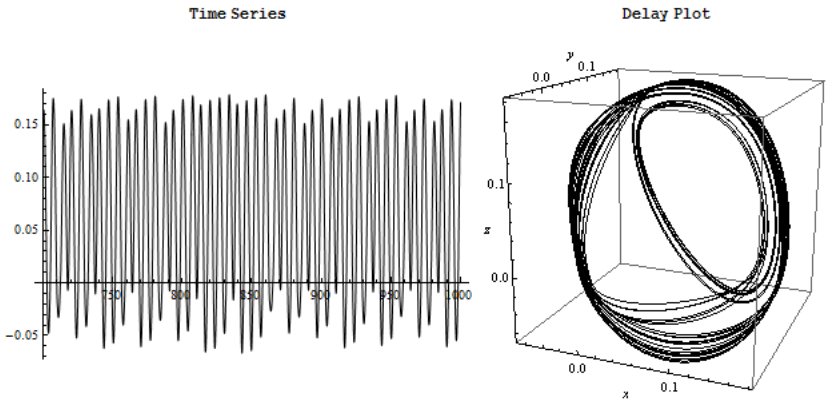

Figure 5.2.1. Time series and delay plot of chaotic symmetric vocal fold model solution

The type of chaos present here bears a certain resemblance to that of the Lorenz oscillator in that it exhibits alternating sections of nearly periodic behavior. Although the time series data almost seems periodic, it is clear from the thick curves in the delay plot that the solution is not actually visiting the exact value but merely coming close. If the delay plot had come from actual periodic data, the result would be much thinner curves. As can be seen in Figure 5.2.2, where time series data of a solution to the two-mass model which exhibits seemingly similar complexity produces a much simpler delay plot. It should also be noted the time series and delay plots in Figure 5.2.2 and 5.2.1 are both constructed from the same number of points.

The spacing of the curves in the delay plot in Figure 5.2.1 is quite similar to that of the Lorenz oscillator's delay plot. Figure 5.2.3 shows a close up of one of the sections of curves in the two-mass models delay plot, while Figure 5.2.4 shows a close up of the Lorenz oscillator's delay plot. There is a noticeable similarity between the two.

Experiments run on the model verified the results found in [6] and [4] that more predominant overtones occur for higher values of P_s. The reason given for this is due to increased

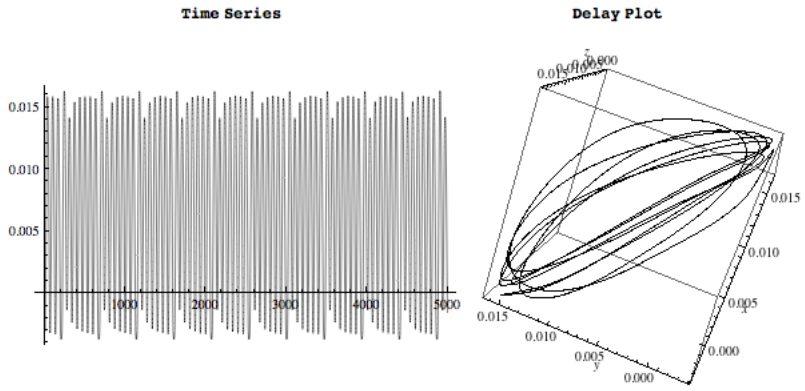

Figure 5.2.2. Time series and delay plot of a periodic symmetric vocal fold model solution

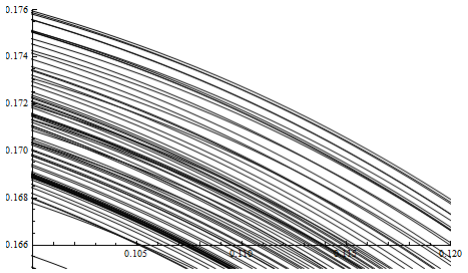

Figure 5.2.3. Close up of symmetric two-mass model chaotic solutions delay plot

collision between the two sets of masses at high forcing pressures. It was also discovered the coupling constant between the two masses k_c produced more overtones for higher values. This was of course very helpful since more overtones suggests period doubling, and as discussed in Section 2.2.2 period doubling suggests the existence of chaos.

5.3 Chaos in the Two-Mass Syrinx Model

The two-mass model of the syrinx from [5] was then implemented into Mathematica. Even for very high values of P_s there were few increases in the amount of overtones when using the default parameters provided. Different values of k_c were tested, and as with the vocal fold version of the two-mass model an increase in the number of overtones was witnessed. With high levels of P_s and k_c, chaos was also observed.

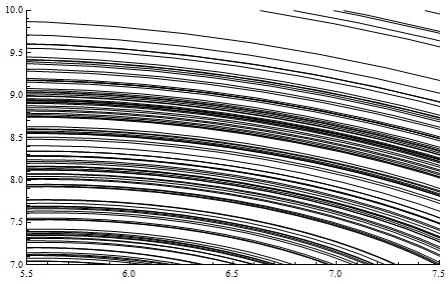

Figure 5.2.4. Close up of Lorenz attractor's delay plot

Figure 5.3.1 shows chaotic time series data from the solution $x(t)$ with changes from the default parameters as follows: $k_c = 0.09$, $P_s = 0.08$, $x_1(0) = x_2(0) = 0.01$, $r_2 = 0.001$. Figure 5.3.2 shows the resulting delay plot from the time series data in Figure 5.3.1.

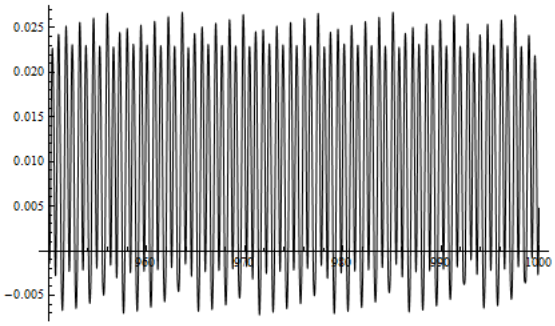

Figure 5.3.1. Chaotic time series data from syrinx model ($k_c = 0.09$, $P_s = 0.08$, $x_1(0) = x_2(0) = 0.01$, $r_2 = 0.001$)

Figure 5.3.3 shows a close up of a delay plot in Figure 5.3.2. Again there is a noticeable similarity between the spacing of the curves in the delay plot constructed from time series data produced by the syrinx model and that of the Lorenz model.

5.4 Discussion on Parameters

It is somewhat difficult to say if the parameters used to obtain the chaotic data in Figure 5.3.2 are realistic parameters for a real bird. It may even be difficult to define what is meant by the idea of realistic parameters for this model. The coupling constant k_c, for

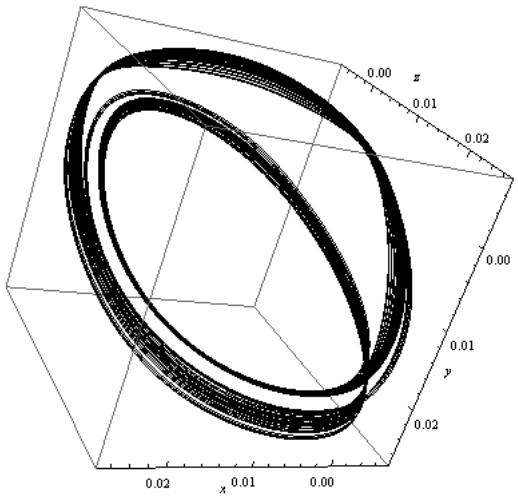

Figure 5.3.2. Delay plot constructed from the times series data seen in Figure 5.3.1

instance, is much higher than the default parameter used. In terms of the labia the model is representing, this would mean there is a stronger connection between its upper and lower portions. In terms of a parameter which has been measured for actual bird anatomy, this idea is harder to quantify. Another point worth making is the fact that there is a fairly large error when measuring parameters relating to such delicate bird anatomy.

The changes made to P_s also could be up for debate. The default parameters model from [5], for example, are for a general songbird. There is however an incredible variance among the anatomy and sizes of songbirds. A second model in [5] is proposed which is specifically shaped to a Ring Dove. For this model the paper refers to .05 as being high for levels of P_s. Therefor a level of $P_s = 0.08$ may be at the top end or possibly a bit over high values of P_s for a bird such as a Ring Dove. It most likely would also be over realistic levels for a Zebra Finch which is smaller than a Ring Dove. However it may be within the realistic values of sub-glottal pressure for a larger bird such as the Sulfur Crested Cockatoo, or a Gang-gang Cockatoo which were both found to have chaotic calls in [9].

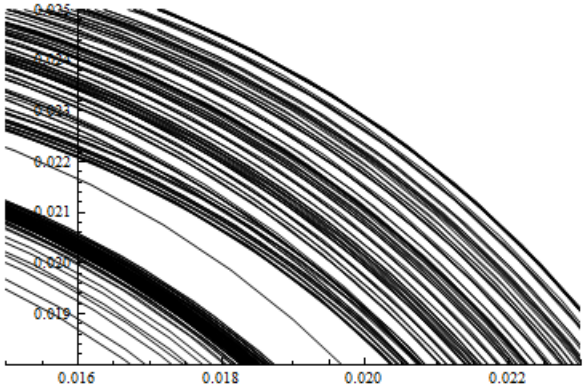

Figure 5.3.3. Close up of delay plot constructed from chaotic time series produced by a solution from one of the differential equations governing syrinx model

A fair conclusion that can be made from the results discussed in Section 5.3 is that there exists chaos in the two-mass model of the syrinx for feasible parameters for some bird species. This is of course only a first step and, time permitting, parameters more specific for a particular bird would have been looked into. As is suggested in [5], for varying values of the damping constant r the model exhibits varying amounts of overtones. Thus it seems likely by varying the r and k_c values it would be possible to induce chaos in the two-mass model for realistic values of P_s for a significant range of different bird species.

A large obstacle that was faced when testing varied parameters for the syrinx model was lack of computing power. For slightly lower values of k_c and P_s, which would have been closer to the default parameters provided by the model, the computers being used were unable to complete the computation. Since Mathematica took longer to finish computations of chaotic solutions compared to periodic solutions it seems likely these parameters would have resulted in chaotic data. However without the results from the computation this can only be offered as speculation.

6
Conclusion

Aperiodic birdsongs of the Zebra Finch were analyzed for chaos using recurrence analysis and delay plots. Although the data was successfully classified as deterministic, further research suggested its behavior was more characteristic of periodic data with noise added in. To investigate if chaos was present in current modeling techniques, a model of the avian sound producing organ, the syrinx, was also analyzed for chaos using delay plot analysis. The model chosen was a re-scaled version of a well known two-mass model of the human vocal folds. The model was found to exhibit chaotic behavior for feasible parameters for birds capable of producing chaotic vocalizations.

Bibliography

[1] Seppo Fagerlund, *Acoustics and physical models of bird sounds*, http://www.acoustics.hut.fi/.

[2] Kathleen T. Alligood, Tim D. Sauer, and James A. Yorke, *Chaos: an introduction to dynamical systems*, Springer-Verlag, New York, 1996.

[3] K Ishizaka and J.L. Flanagan, *Synthesis of voiced sounds from a two-mass model of the vocal cords*, Bell. Syst. Tech. **51** (1972), 1233–1268.

[4] Ina Steineche and Hanspeter Herzel, *Bifurcations in an asymmetric vocal fold*, Acoustical Society of America **97** (1995), 1874–1884.

[5] Hanspeter Herzel, Riccardo Zeccarelli, Coen Elemans, and Tecumsch Fitch, *Two-Mass Models of Bird Syrinx*, Models and Analysis of Vocal Emissions for Biodmedical Applications: 4th International Workshop [Proceedings] **110** (2005), 2120–2128.

[6] Yu Zhang, Jack J. Jiang, and Jennifer Stern, *Modeling of chaotic vibrations in symmetric vocal folds*, Acoustical Society of America **110** (2001), 2120–2128.

[7] Tijana T. Ivancevic, *Computational mind: a complex dynamics perspective*, Springer, New York, 2007.

[8] Michale S. Fee, Boris Shraiman, Bijan Pesaran, and Partha P. Mitra, *The role of nonlinear dynamics of the syrinx in the vocalizations of a songbird*, Nature **395** (1998), 67–71.

[9] N.H. Fletcher, *A class of chaotic bird calls?*, J. Acoust. Soc. Am. **108** (2000), 821–826.

[10] S. Horai, T. Yamada, and K. Aihara, *Determinism analysis with isodirectional recurrence plots*, IEEE Trans. Inst. Electric. Eng. Jpn. **C 122 (1)** (2007), 141–147.

[11] I. Aihara, H. Kitahata, S. Horai, K. Aihara, and K. Yoshikawa, *Dynamical calling behavior experimentally observed in Japanese tree frogs (Hyla Japonica)*, IEIC Trans. Fundamentals **E90-A** (2007).

[12] Mary L. Leonardi, *Prediction and Geometry of Chaotic Time Series*, 1997, `http://www.dtic.mil`.

[13] Heather H. Williams, *(1997) Zebra Finch Song Archive*, `http://wso.williams.edu/~hwilliam/ZFsongs/`.

[14] *Recurrence Plots and Cross Recurrence Plots*, `http://www.recurrence-plot.tk/`.

[15] N. Marwan, M.C. Romano, M. Thiel, and J. Krths, *Recurrence Plots for the Analysis of Complex Systems*, Physics reports **438(5-6)**, 237-329.